EUROPEAN ORGANIZATION FOR NUCLEAR RESEARCH

CERN-EP/89-07
January 17th, 1989

Test of QCD and a Measurement of Λ from Scaling Violations in the Proton Structure Function $F_2(x,Q^2)$ at High Q^2

BCDMS Collaboration

A.C. Benvenuti, D. Bollini, G. Bruni, L. Monari[1] and F.L. Navarria
Dipartimento di Fisica dell'Università and INFN, Bologna, Italy

A. Argento[2], J. Cvach[3], W. Lohmann[4], L. Piemontese[5], G. Todorova[6] and P. Zavada[3]
CERN, Geneva, Switzerland

A.A. Akhundov, V.I. Genchev, V.G. Krivokhizhin, V.V. Kukhtin, R. Lednicky, S. Nemecek, P. Reimer, I.A. Savin, N.B. Skachkov, A.V. Sidorov, G.I. Smirnov, J. Strachota[3], G. Sultanov[7], P. Todorov[7] and A.G. Volodko
Joint Institute for Nuclear Research, Dubna, USSR

D. Jamnik[8], R. Kopp[9], U. Meyer-Berkhout, A. Staude, K.-M. Teichert, R. Tirler[10], R. Voss[11] and C. Zupancic
Sektion Physik der Universität, München, Federal Republic of Germany[12]

M. Cribier, J. Feltesse, A. Milsztajn, A. Ouraou, Y. Sacquin, G. Smadja and M. Virchaux
DPhPE, CEN Saclay, France

Abstract

Scaling violations in the proton structure function $F_2(x,Q^2)$ measured with high statistics in deep inelastic scattering of muons on a hydrogen target are compared to predictions of perturbative QCD. Excellent agreement is observed with numerical solutions of the evolution equations in leading and next-to-leading order. The QCD mass scale parameter Λ is determined from these data both in a flavour nonsinglet approximation and with a complete flavour singlet and nonsinglet treatment. An estimate of the gluon distribution in the proton is given.

Submitted to Physics Letters B

---

[1] Deceased.

[2] Now at Digital Equipment, Torino, Italy.

[3] On leave from Institute of Physics, CSAV, Prague, Czechoslovakia.

[4] On leave from the Institut für Hochenergiephysik der AdW der DDR, Berlin-Zeuthen, GDR.

[5] Now at INFN, Ferrara, Italy.

[6] Now at the Institute of Mathematics, Bulgarian Academy of Sciences, Sofia, Bulgaria.

[7] Now at the Institute of Nuclear Research and Nuclear Energy, Bulgarian Academy of Sciences, Sofia, Bulgaria.

[8] On leave from E. Kardelj University and the J. Stefan Institute, Ljubljana, Yugoslavia.

[9] Now at Siemens AG, Munich, Germany.

[10] Now at DPhPE, CEN Saclay, France.

[11] Now at CERN, Geneva, Switzerland.

[12] Funded in part by the German Federal Minister for Research and Technology (BMFT) under contract number 054MU12P6.

In a previous letter [1], we have reported on a high statistics measurement of the proton structure function $F_2(x,Q^2)$ at large four-momentum transfer Q^2 in deep inelastic scattering of muons on a hydrogen target. These data exhibit clear deviations from Bjorken scaling. Here we compare the measured scaling violations to predictions from perturbative Quantum Chromodynamics (QCD). The results of a similar analysis of the nucleon structure function measured with a carbon target have been reported earlier [2,3,4]. Tests of QCD from earlier high statistics muon and neutrino experiments are reported on in refs. [5 – 12].

In the framework of perturbative QCD [13], scaling violations are due to the Q^2 evolution of quark and gluon distributions which can be described by the Altarelli-Parisi equations [14] or, alternatively, by the Q^2 dependence of their moments [15]. Higher twist contributions to F_2, which are not described by these equations, vary like power series in $1/Q^2$ [16] and are expected to be small over most of the Q^2 range of our data. Furthermore, the data extend up to $x = 0.75$, thus requiring only little extrapolation to calculate the evolution integrals. Our measurement is therefore well suited to a precise test of perturbative QCD.

Several numerical methods have been proposed to fit the QCD predictions to experimental data. We have mainly employed two methods [4,17,18,19] which have been developed within our collaboration. They allow to fit the flavour singlet and nonsinglet evolution equations both in a leading order (LO) perturbation expansion and in a next-to-leading order expansion in the $\overline{\text{MS}}$ renormalization scheme. Four quark flavours were assumed throughout the QCD analysis.

The experimental data shown in Fig. 2 of ref. [1] were used for the fits. Data points with $y < 0.20$ at $x = 0.75$, $y < 0.16$ at $x = 0.65$ and $y < 0.14$ in all other bins of x were excluded to reduce the sensitivity of the fits to systematic uncertainties. Points with $Q^2 < 8$ GeV^2 at $x < 0.16$, $Q^2 < 14$ GeV^2 at $0.16 < x < 0.25$, and with $Q^2 < 20$ GeV^2 at $x > 0.25$ were excluded to suppress possible higher twist effects. The combined data after these cuts are shown in Fig. 1.

In the nonsinglet approximation, the gluon contribution is neglected in the evolution equations. Estimates of the gluon distribution from muon [3,5,6] and neutrino scattering experiments [8,9] have shown that this approximation is valid at high values of the scaling variable x. Therefore, in the nonsinglet analysis of the data reported here, only the kinematic region with $x \geq 0.275$ was considered.

The cut at $Q^2 < 20\ GeV^2$ further reduces the contribution of the gluon distribution which becomes softer with increasing Q^2 due to its QCD evolution. The results of these fits are summarized in Table 1. We find good agreement between the values of Λ obtained with the different programs. The average result for the QCD mass scale parameter in next-to-leading order is

$$\Lambda_{\overline{MS}} = 205 \pm 22\ (stat.) \pm 60\ (syst.)\ MeV,$$

corresponding to a strong coupling constant of

$$\alpha_S(Q^2 = 100\ GeV^2) = 0.156 \pm 0.004\ (stat.) \pm 0.011\ (syst.).$$

To evaluate the systematic errors on Λ and α_S, the individual systematic uncertainties on F_2 were added to the data and the fits repeated. This was done for each contribution to the systematic error in turn and the resulting changes in Λ were combined in quadrature. The final systematic error $\Delta\Lambda = 60$ MeV is dominated by the 1% uncertainty on the relative normalization between data taken at the four different beam energies. We have checked that all numerical results on Λ and α_S presented in this paper are insensitive to the choice of the Q_0^2 at which the QCD evolution is started.

Global QCD fits as they are conventionally used to determine Λ do not, however, constitute a sensitive test of Quantum Chromodynamics. In general, the χ^2's of such fits describe mainly their agreement with the x dependence of the structure functions which is not predicted by the theory, and the fits can be biased by a priori assumptions on the functional form of $F_2(x,Q_0^2)$. A more stringent test is obtained by comparing directly the x dependence of the measured scaling violations, averaged over Q^2, to the one expected from the QCD evolution. Within the accuracy of the present measurements, this is the only specific prediction of perturbative QCD for deep inelastic scattering which can be tested experimentally. In the nonsinglet approximation, this comparison depends on Λ as the sole free parameter whereas in a singlet analysis over the full x range it is also sensitive to the gluon distribution.

The nonsinglet case is shown in Fig. 2a where the logarithmic derivatives $d\ln F_2(x,Q^2)/d\ln Q^2$ are compared to the next-to-leading order prediction for $\Lambda_{\overline{MS}} = 205$ MeV. The logarithmic derivatives in this figure are the slope parameters of straight line fits $\ln F_2 = a \cdot \ln Q^2 + b$ to the data. To calculate

in a consistent way the theoretical predictions shown in the same figure, the result of the QCD fit, F_2^*, was assigned at each (x,Q^2) point the statistical error of the corresponding experimental F_2. The logarithmic derivatives $d\ln F_2^*/d\ln Q^2$ were then obtained by the same straight line fit as for the experimental data. Within the errors, this linear representation is an excellent approximation of both the experimental and the predicted Q^2 evolution. The measured x dependence of the scaling violations in Fig. 2a is in agreement with the predicted one within statistical errors.

For the QCD analysis over the full x range of the data, the proton structure function is decomposed into a singlet (S) and a nonsinglet (NS) part as $F_2 = F_2^S + F_2^{NS}$ where F_2^{NS} and F_2^S follow different Q^2 evolutions, the evolution of F_2^S being coupled to the gluon distribution. We have checked using the method of ref. [20] that the effect of the charm threshold is negligible in the kinematic range of this analysis.

The usual method to determine the gluon momentum distribution is to parametrize it at a given Q_0^2 and to evolve it with Q^2. We have chosen the parametrization $xG(x,Q_0^2) = A(\eta+1)(1-x)^\eta$ at $Q_0^2 = 5\ GeV^2$. A more complicated parametrization is not justified by the accuracy of our measurement. The parameters A and η have been fitted together with Λ and with parametrizations of F_2^{NS} and F_2^S. The results obtained with our two fitting programs are in good agreement and are given in Table 2. The results for Λ agree with those of the nonsinglet fits. In next-to-leading order, we find a soft gluon distribution which justifies the nonsinglet fits of $\Lambda_{\overline{MS}}$ discussed above. Systematic errors on Λ and η have been evaluated as for the nonsinglet case.

Assuming the parametrization of $xG(x,Q_0^2)$ to be valid over the full x range, A equals the fraction of the proton momentum carried by the gluons. When it is treated as a free parameter in the fits, we find $A \approx 0.5$. This is compatible with what is expected from the momentum sum rule which we have therefore imposed in the following analysis in order to constrain A. The results from such fits are given in Table 3 and are in good agreement with those quoted in Table 2. We have also used the program of ref. [18] to calculate for fixed values of η the χ^2 of the comparison of measured and predicted logarithmic derivatives of F_2 in the same way as for the nonsinglet fits. These χ^2's are shown in Fig. 3a and exhibit different minima for the leading and next-to-leading order fits. Λ and η corresponding to these minima coincide with the results given in Table 3. The correlation between η and Λ is shown in

Fig. 3b and is weaker than observed in previous experiments. This is a consequence of the softness of the gluon distribution and of the high accuracy of the data at large x where the effect of the gluons becomes negligible. The measured scaling violations are compared in Fig. 3c to next-to-leading order fits for different values of η and show again very good agreement with the theoretical prediction for $\eta = 8.3$. Higher twist effects are thus not required to explain the scaling violations observed in our data.

The gluon distributions in leading and next-to-leading order which correspond to the fits of Table 2 are shown in Fig. 4. They are valid only in the range $0.06 \leq x \leq 0.30$ since there are no F_2 data at smaller x, and at large x the gluon distribution is too small to have a noticeable effect on the scaling violations. Also shown in the same figure is the earlier EMC result [5] obtained in leading order for a fixed value of $\Lambda = 90$ MeV.

A complementary method to determine the gluon momentum distribution consists in evaluating it from the measured scaling violation in each bin of x separately. When the QCD mass scale parameter is fixed, the gluon distribution is the only unknown function in the QCD evolution equation. It is estimated at each bin center x_i individually by assuming a parametrization for $xG(x,Q_0^2)$ at $x \geq x_i$, which we take to be

$$xG_i(x,Q_0^2) = C_i[(1-x)/(1-x_i)]^{\zeta} \qquad (x \geq x_i),$$

using only the scaling violations measured at $x = x_i$ and assuming $\Lambda_{\overline{MS}} = 220$ MeV (see below). The coefficients $C_i = x_i G_i(x_i,Q_0^2)$ are fitted separately using the same value for ζ. This parameter is determined iteratively such that the x dependence of the fitted C_i's is well described by a parametrization proportional to $(1-x)^{\zeta}$. In next-to-leading order, the best agreement is observed for $\zeta = 11$ as expected from the previous method. Assuming $\zeta = 9$ ($\zeta = 13$) decreases (increases) all C_i's by approximately 8%. The principal interest of this method lies in the reliable estimate of statistical errors. The coefficients C_i for $\zeta = 11$ are shown in Fig. 4 together with the fits of $xG(x,Q_0^2)$ given in Table 2. The dominant systematic error is due to the relative normalisation uncertainty, whereas the uncertainty on $\Lambda_{\overline{MS}}$ has only a negligible effect. The total systematic errors, including the uncertainty on ζ, are typically half the statistical ones.

The QCD analysis presented in this paper can be compared to the one performed on our earlier measurement with a carbon target [3]. The kinematical domains used for the nonsinglet fits are almost identical and the results for Λ are in agreement within statistical errors. They can be combined to give

$$\Lambda_{\overline{MS}} = 220 \pm 15 \text{ (stat.)} \pm 50 \text{ (syst.) MeV}$$

corresponding to a strong coupling constant

$$\alpha_s(Q^2 = 100 \text{ GeV}^2) = 0.1585 \pm 0.0025 \text{ (stat.)} \pm 0.0090 \text{ (syst.)}.$$

The largest contributions to the systematic errors on the two measurements of $\Lambda_{\overline{MS}}$ come from the normalization uncertainties between data taken at different beam energies. These uncertainties are to a large extent uncorrelated between the carbon and hydrogen experiments, thus allowing to reduce the systematic error from this contribution for the combined result. The scaling violations measured with the two different targets are compared in Fig. 2b to their respective QCD prediction for the same value of $\Lambda_{\overline{MS}} = 220$ MeV. Different scaling violations in hydrogen and carbon are predicted by the evolution equation from the different x dependence of F_2 measured on proton and isoscalar targets. Such a difference is observed in the data with a good statistical significance: the probability $P(\chi^2)$ of the carbon and hydrogen data to agree with their respective QCD prediction is 40%, whereas the combined probability of the carbon data to agree with the hydrogen prediction and of the hydrogen data to agree with the carbon prediction is less than 0.3%. We estimate the latter probability to increase to a few percent when systematic errors are taken into account. The fact that different patterns of scaling violation are compatible with a common value of $\Lambda_{\overline{MS}}$ is an additional confirmation of the remarkable consistency between our data and the QCD predictions.

In conclusion, we find that scaling violations observed in our high statistics measurement of the proton structure function $F_2(x,Q^2)$ at high Q^2 are in quantitative agreement with predictions from perturbative QCD. Nonperturbative effects are not required to explain scaling violations in the kinematic range of this experiment. The nonsinglet approximation and the complete singlet and nonsinglet fits to the data give consistent results for $\Lambda_{\overline{MS}}$ which are in agreement with our earlier result from a carbon target. Combining these measurements, we obtain a value of $\Lambda_{\overline{MS}} = 220 \pm 15 \pm 50$ MeV. The

gluon distribution of the proton has been determined from singlet + nonsinglet fits in next-to-leading order QCD in the range $0.06 \leq x \leq 0.30$.

References

[1] BCDMS, A.C. Benvenuti et al., CERN-EP/89−06, submitted to Physics Letters B.

[2] BCDMS, A.C. Benvenuti et al., Phys. Lett. 195B (1987) 91.

[3] BCDMS, A.C. Benvenuti et al., Phys. Lett. 195B (1987) 97.

[4] M. Virchaux, Thèse, Université Paris VII, 1988.

[5] EMC, J.J. Aubert et al., Nucl. Phys. B259 (1985) 189.

[6] EMC, J.J. Aubert et al., Nucl. Phys. B272 (1986) 158.

[7] BFP, P.D. Meyers et al., Phys. Rev. D34 (1986) 1265.

[8] CDHS, H. Abramowicz et al., Z. Phys. C17 (1983) 283.

[9] CHARM, F. Bergsma et al., Phys. Lett. 123B (1983) 269 and Phys. Lett. 153B (1985) 111.

[10] CCFRR, D.B. MacFarlane et al., Z. Phys. C26 (1984) 1.

[11] BEBC−WA25, D. Allasia et al., Phys. Lett 135B (1984) 231 and Z. Phys. C28 (1985) 321.

[12] BEBC−WA59, K. Varvell et al., Z. Phys. C36 (1987) 1.

[13] For extensive reviews of perturbative QCD and further references, see: A. Buras, Rev. Mod. Phys. 52 (1980) 199; G. Altarelli, Phys. Rep. 81 (1982) 1.

[14] G. Altarelli and G. Parisi, Nucl. Phys. B126 (1977) 298.

[15] For a review, see D.W. Duke and R.G. Roberts, Phys. Rep. 120 (1985) 275.

[16] See e.g. R.K. Ellis, W. Furmanski and R. Petronzio, Nucl. Phys. B212 (1983) 29.

[17] A. Ouraou, Thèse, Université Paris XI, 1988.

[18] M. Virchaux and A. Ouraou, Preprint DPhPE 89-07, in preparation.

[19] V.G. Krivokhizhin et al., Z. Physik C 36 (1987) 51.

[20] M. Glück, E. Hoffmann and E. Reya, Z. Phys. C 13 (1982) 119; S.P. Luttrell and S. Wada, Nucl. Phys. B182 (1981) 381.

Table Captions

Table 1: Results of nonsinglet QCD fits to $F_2(x,Q^2)$ in leading order (LO) and next-to-leading order in the $\overline{MS}$ renormalisation scheme. The data are fitted in the kinematic range $x \geq 0.275$ and $Q^2 \geq 20$ GeV^2; additional cuts on y are discussed in the text. Four quark flavours are assumed in the QCD analysis. χ^2_S is the χ^2 of the direct comparison between measured and predicted scaling violations (Fig. 2a). Only statistical errors are given.

Table 2: Results of singlet + nonsinglet QCD fits to $F_2(x,Q^2)$ over the full x range of the data, in leading order (LO) and next-to-leading order in the $\overline{MS}$ renormalisation scheme, without imposing the momentum sum rule. Kinematic cuts are discussed in the text. A and η are the parameters of the gluon momentum distribution which is chosen as $xG(x) = A(\eta+1)(1-x)^{\eta}$. Four quark flavours are assumed in the QCD analysis. Only statistical errors are given.

Table 3: As Table 2, but imposing the momentum sum rule.

Table 1: Results of nonsinglet QCD fits to $F_2(x,Q^2)$.

Method	Λ_{LO} (MeV)	χ^2/DOF	χ^2_S/DOF	$\Lambda_{\overline{MS}}$ (MeV)	χ^2/DOF	χ^2_S/DOF
Ref. [18]	178±22	180/198	7.8/5	208±22	177/198	6.1/5
Ref. [19]	181±21	180/198	7.9/5	198±21	177/198	4.7/5
Carbon target [3]	210±20			230±20		

Table 2: Singlet+nonsinglet QCD fits to $F_2(x,Q^2)$ without imposing the momentum sum rule.

Method	Ref. [18]	Ref. [19]
Λ_{LO} (MeV)	200 ± 30	210 ± 35
A_{LO} (Q^2 = 5 GeV^2)	0.61 ± 0.12	0.59 ± 0.10
η_{LO} (Q^2 = 5 GeV^2)	5.8 ± 2.5	4.8 ± 2.2
χ^2/DOF	254/268	257/269
χ^2_S/DOF	11.7/8	12.5/8
$\Lambda_{\overline{MS}}$ (MeV)	214 ± 22	207 ± 23
$A_{\overline{MS}}$ (Q^2 = 5 GeV^2)	0.62 ± 0.20	0.58 ± 0.10
$\eta_{\overline{MS}}$ (Q^2 = 5 GeV^2)	11.6 ± 3.0	8.5 ± 2.3
χ^2/DOF	256/268	256/269
χ^2_S/DOF	8.6/8	10.7/8

Table 3: *Singlet + nonsinglet QCD fits to $F_2(x,Q^2)$, imposing the momentum sum rule.*

Method	Ref. [18]	Ref. [19]
Λ_{LO} (MeV)	215 ± 27	216 ± 30
η_{LO} (Q^2 = 5 GeV^2)	3.7 ± 1.2	4.2 ± 1.5
χ^2/DOF	257/269	257/270
χ^2_S/DOF	15.2/9	13.4/9
$\Lambda_{\overline{MS}}$ (MeV)	224 ± 21	212 ± 21
$\eta_{\overline{MS}}$ (Q^2 = 5 GeV^2)	8.3 ± 1.5	7.8 ± 1.5
χ^2/DOF	258/269	256/270
χ^2_S/DOF	11.4/9	11.5/9

Figure captions

Fig. 1: The structure function $F_2(x,Q^2)$ using $R = R_{QCD}$ for all beam energies combined. The solid lines represent the singlet + nonsinglet QCD fit discussed in the text. Only statistical errors are shown.

Fig. 2: (a) The logarithmic derivatives $d\ln F_2(x,Q^2)/d\ln Q^2$ observed in this experiment at $Q^2 > 20$ GeV^2 and $x \geq 0.275$. The inner error bars are statistical, the outer error bars show statistical and systematic errors added linearly. The systematic errors are strongly correlated. The lines show nonsinglet QCD predictions for $\Lambda_{\overline{MS}} = 205$ MeV and for two other values of Λ.

(b) As (a), compared to carbon target results obtained with the same apparatus [3]. The QCD predictions are shown for a common value of $\Lambda_{\overline{MS}} = 220$ MeV. Only statistical errors are shown. The systematic errors of the carbon data are very similar to those of the hydrogen data shown in (a).

Fig. 3: (a) The χ^2 of the comparison of measured and predicted scaling violations as a function of the exponent η of a gluon distribution $xG(x,Q_0^2) = A(\eta+1)(1-x)^\eta$ at $Q_0^2 = 5$ GeV^2 from flavour singlet + nonsinglet fits at leading and next-to-leading order.

(b) The dependence of the QCD mass scale parameter Λ on the exponent η of the gluon distribution from the same fits as in (a).

(c) The same as Fig. 2a, but for the full kinematical range of the data. The singlet + nonsinglet prediction in next-to-leading order QCD is also shown for different exponents η.

Fig. 4: The gluon momentum distribution $xG(x,Q_0^2)$ in the proton at $Q_0^2 = 5$ GeV^2. The parametrizations shown correspond to the results of the QCD fits in leading and next-to-leading order from Table 2 and are compared to the earlier leading order analysis from the EMC experiment [5]. Also shown is the gluon distribution determined in bins of x as discussed in the text. No systematic errors are shown.

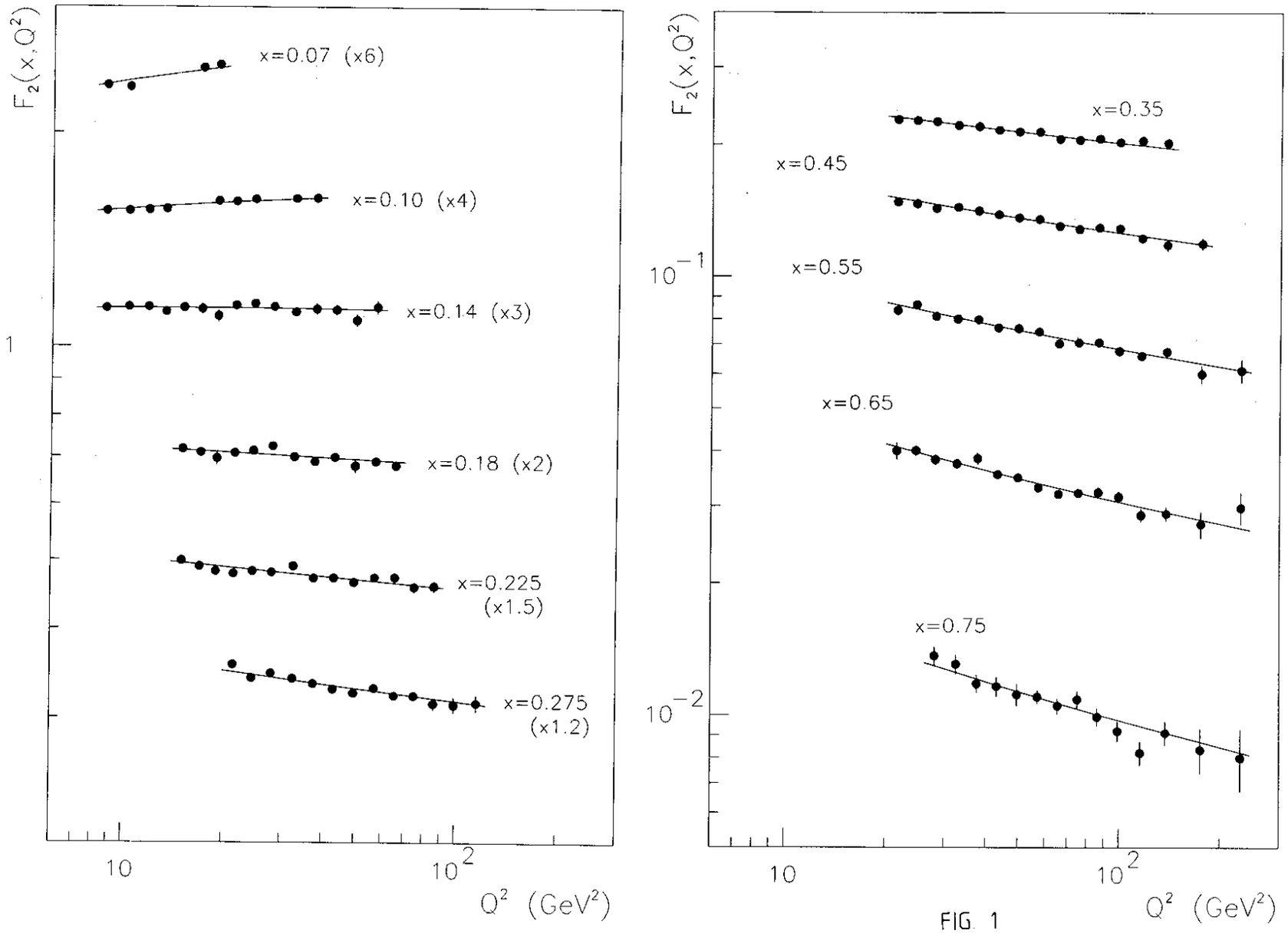
$F_2(x,Q^2)$
x=0.07 (x6)
x=0.10 (x4)
x=0.14 (x3)
x=0.18 (x2)
x=0.225
(x1.5)
x=0.275
(x1.2)
1
10
10^2
Q^2 (GeV^2)
$F_2(x,Q^2)$
x=0.35
x=0.45
x=0.55
x=0.65
x=0.75
10^{-1}
10^{-2}
10
10^2
Q^2 (GeV^2)

FIG. 1

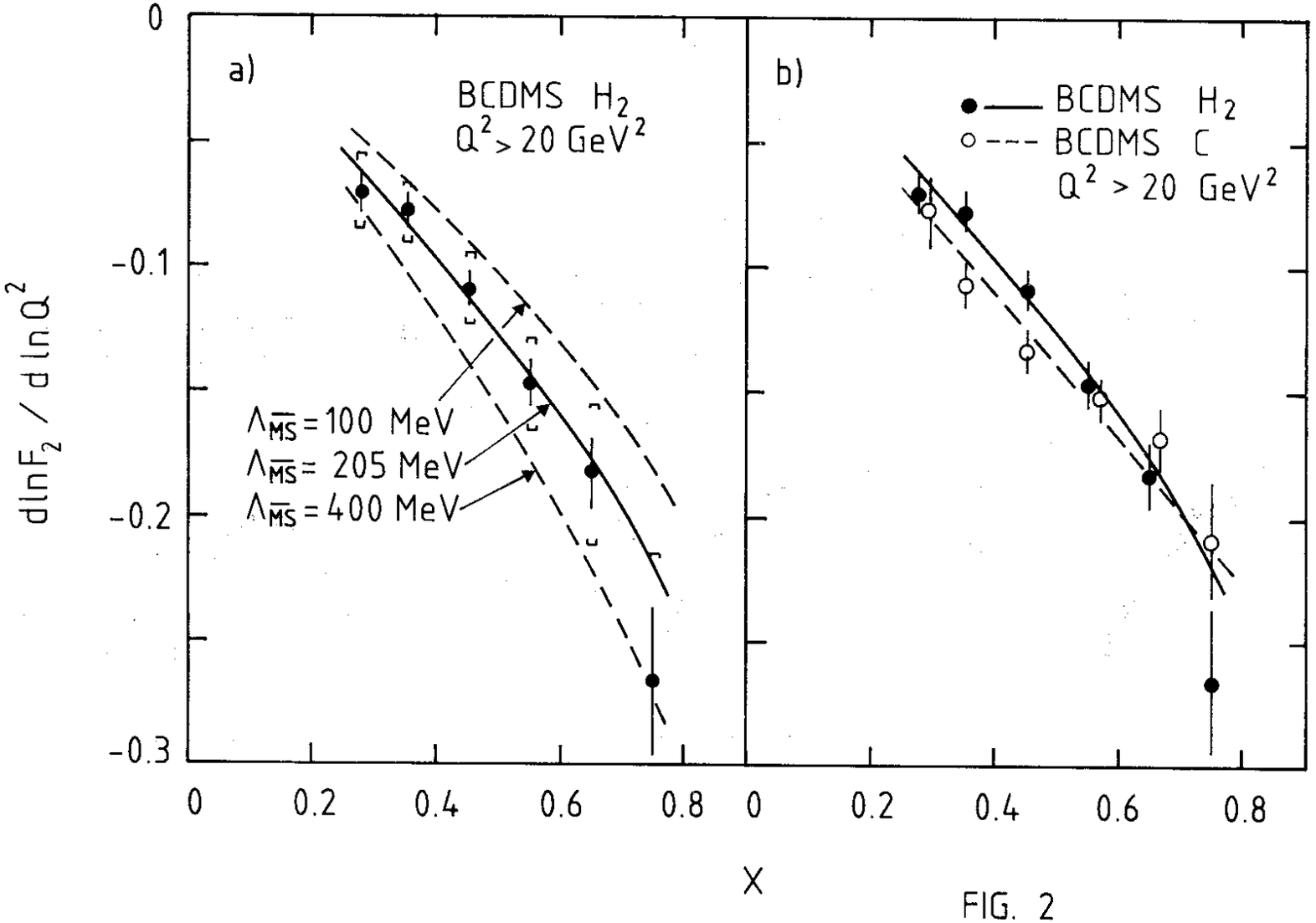
a)
BCDMS H_2
$Q^2 > 20\ GeV^2$
$\Lambda_{\overline{MS}} = 100$ MeV
$\Lambda_{\overline{MS}} = 205$ MeV
$\Lambda_{\overline{MS}} = 400$ MeV
b)
BCDMS H_2
BCDMS C
$Q^2 > 20\ GeV^2$
$d\ln F_2 / d\ln Q^2$
X
0
-0.1
-0.2
-0.3
0.2
0.4
0.6
0.8

FIG. 2

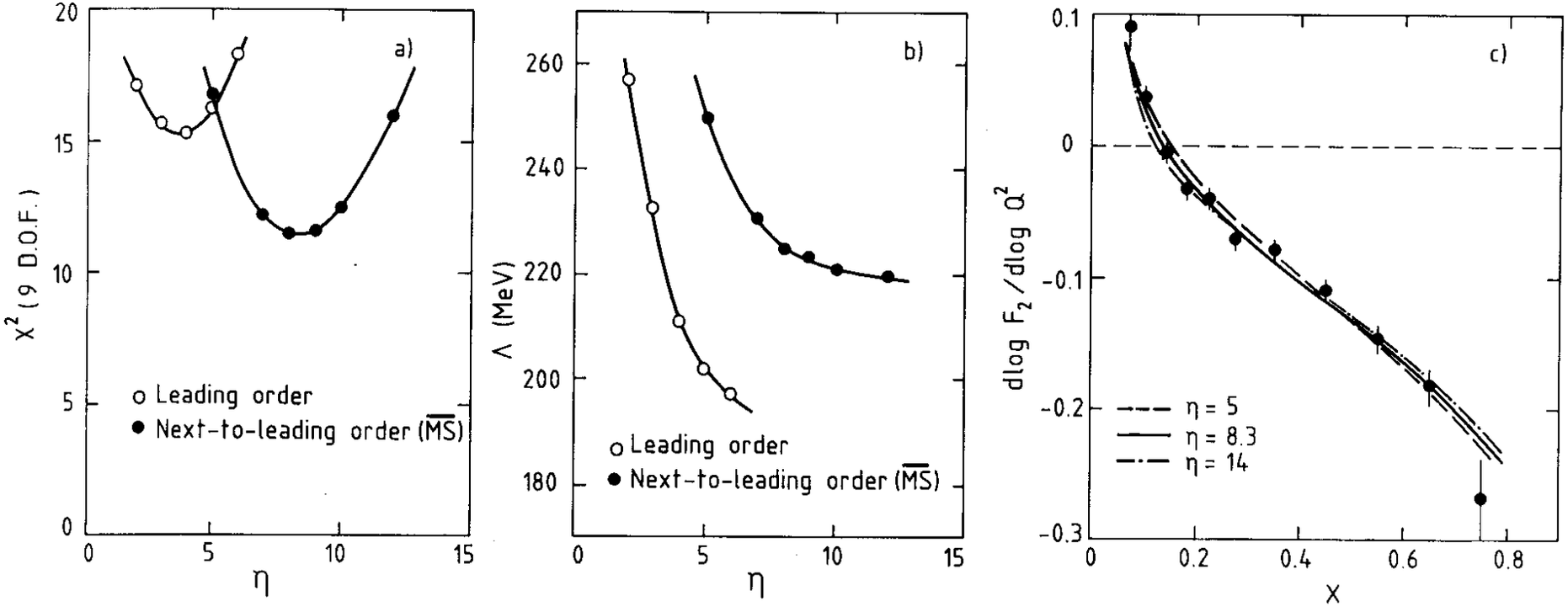
a)
χ^2 (9 D.O.F.)
η
o Leading order
● Next-to-leading order ($\overline{MS}$)
b)
Λ (MeV)
η
o Leading order
● Next-to-leading order ($\overline{MS}$)
c)
dlog F_2 / dlog Q^2
x
η = 5
η = 8.3
η = 14

FIG. 3

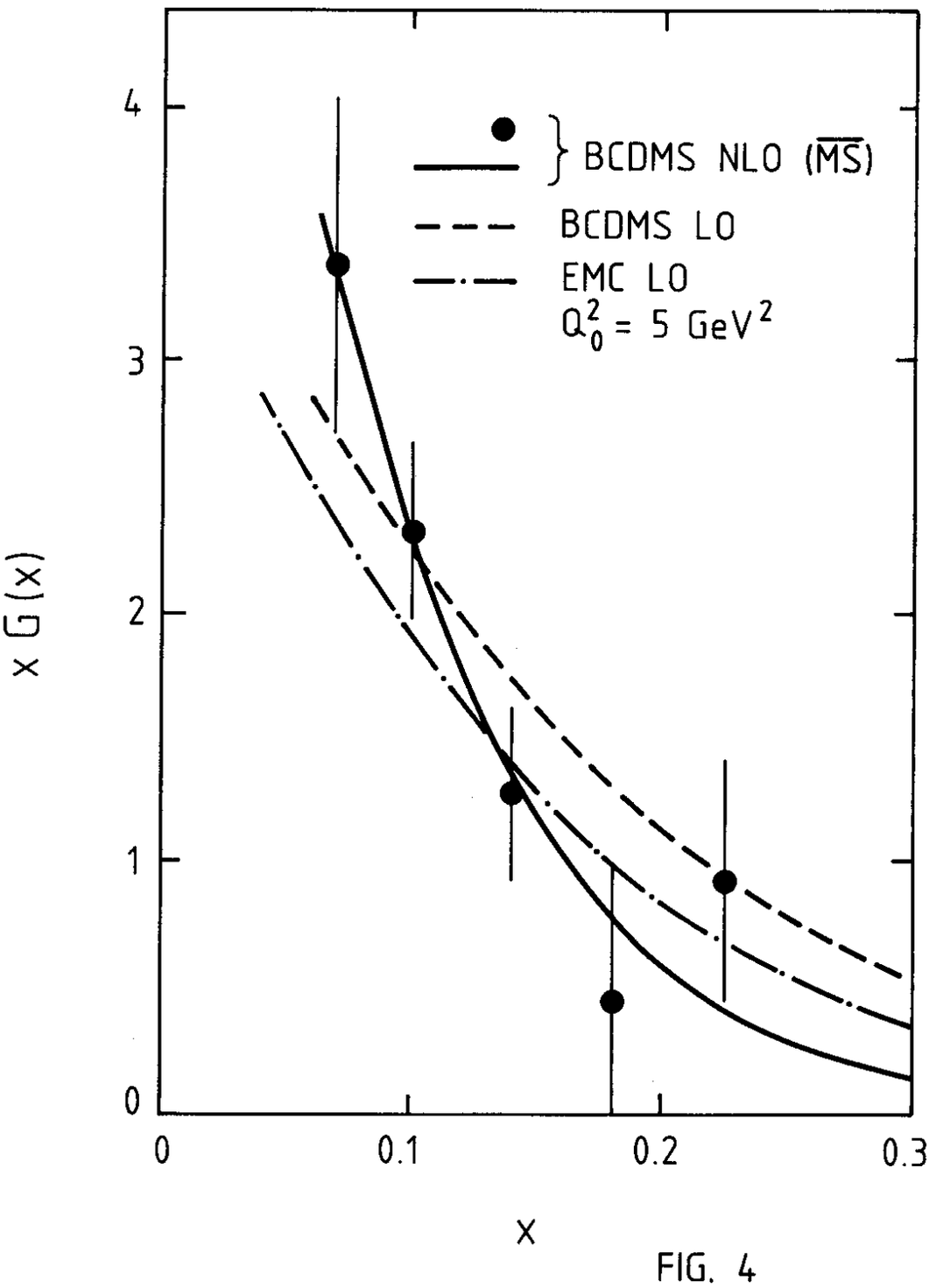

FIG. 4